Nominal Direction and Direction Spread Estimation for Slightly Distributed Scatterers using the SAGE Algorithm

Yin, Xuefeng; Fleury, Bernard Henri

Published in:
IEEE 61st Vehicular Technology Conference, 2005. VTC 2005-Spring. Vol 1

DOI (link to publication from Publisher):
10.1109/VETECS.2005.1543242
10.1109/VETECS.2005.1543242

Publication date:
2005

Document Version
Publisher's PDF, also known as Version of record

Nominal Direction and Direction Spread Estimation for Slightly Distributed Scatterers using the SAGE Algorithm

Xuefeng Yin*, Bernard H. Fleury*

*Information and Signals Division, Department of Communication Technology,
Aalborg University, DK-9220 Aalborg, Denmark
Phone + 45 96 35 86 72, Fax: + 45 98 15 15 83, E-mail: xuefeng@kom.auc.dk

***Abstract*— In this paper, the SAGE (Subspace-Alternating Generalized Expectation-maximization) algorithm [1] [2] is derived using the generalized array manifold (GAM) model proposed in [3] (GAM-SAGE) to estimate the nominal directions, i.e. azimuths and elevations of slightly distributed scatterers (SDSs). As byproducts estimates of the azimuth spreads (ASs), elevation spreads (ESs), and the azimuth-elevation correlation coefficients (AECCs) of the SDSs can be computed from the estimates of the GAM parameters. These parameters determine with close accuracy the direction spreads [4] of SDSs.**

Simulation studies show that in a single-SDS scenario, the GAM-SAGE algorithm outperforms the Spread-ESPRIT technique, and both of them outperform the SAGE algorithm derived with the conventional specular-scatterer (SS) model (SS-SAGE) when the output signal-to-noise ratio (SNR) is beyond a certain threshold which depends on the AS and ES of the SDS. In a two-SDS scenario with strong power unbalance between the SDSs, provided the direction spacing between the SDSs equals twice the intrinsic azimuth or elevation resolution of the array, the GAM-SAGE algorithm can estimate the nominal direction of the SDS with weakest power with tolerably small errors. The SS-SAGE algorithm returns high root mean squared estimation error (RMSEE) regardless of the direction separation.

We also found that the AECC estimator needs to operate in high SNR in order for its bias and RMSEE to be tolerably small. The performance of the AECC estimator, as well as the AS and ES estimators can be improved by applying an array-size selection technique proposed in [5].

I. Introduction

Conventional direction, i.e. azimuth and elevation, of arrival (DoA) estimators are derived based on the specular-scatterer (SS) model which assumes point scattering in the propagation environment. In a scenario where a scatterer has a certain geometrical extent that is small in the view of the receiver (Rx) or local scattering around a transmitter (Tx) located far away from the Rx occurs, the contribution to the received signal can be conceived as the sum of the contributions of multiple sub-scatterers with slightly different DoAs [3] [6] [4]. We refer to such scatterers or clusters of local scatterers as slightly distributed scatterers (SDSs).

It has been shown in [7] that, in propagation environments with SDSs the DoA estimators derived based on the SS model generate estimation errors with a heavy-tailed probability distribution function. This indicates that large estimation errors might happen with high probability. As alternatives, estimators based on approximation models characterizing the signal contribution of SDSs have been proposed. One of the models is the generalized array manifold (GAM) model [3]. In the same reference, three estimators for the nominal DoA (NDoA) of SDSs have been derived based on subspace-based techniques. Application of these methods requires a common prerequisite, i.e. the propagation environment has to be time-invariant. Another approximation model is the two-ray model proposed in [6]. In this reference, the Spread-F technique is reported, which can estimate the NDoAs and angular spreads of SDSs using uniform linear arrays (ULAs) in time-variant environments.

In this paper we derive the SAGE algorithm based on a deterministic version of the GAM model (GAM-SAGE) for estimation of the nominal DoAs, i.e. nominal azimuths and elevations of arrival (NAoAs, NEoAs) of multiple SDSs. The term “deterministic” emphasizes that the (unknown) parameters of the underlying signal model are assumed to be deterministic. The algorithm is derived with the assumptions that the propagation environment is time-variant and the transmitted signal is known to the Rx. The used arrays can have arbitrary layouts and characteristics. The algorithm can be applied with slight modifications in time-invariant environments when the transmitted signal is unknown. As byproducts estimates of the azimuth spreads (ASs), elevation spreads (ESs) and azimuth-elevation correlation coefficients (AECCs) of the SDSs can be computed from the estimates of the parameters in the GAM model. These three parameters exactly characterize with close accuracy the direction spread (DS) [4] of the SDS. Application of the pro-

This work has been conducted in cooperation with Elektrobit Oy, Finland. It has been also partly supported by the Network of Excellence (NEWCOM).

posed GAM-SAGE algorithm for estimation of nominal direction of departure and direction of departure spread is straightforward. Furthermore, when multiple-input multiple-output (MIMO) systems or techniques are considered, the algorithm can be extended to include the nominal directions and direction spreads of the SDSs at both Tx and Rx sites.

The organization of the paper is as follows. Section II and III describe respectively the signal model and the proposed estimators. Section IV reports the simulation results. Finally concluding remarks are addressed in Section V.

II. Signal model

In a propagation scenario with a single SDS the output signal of a M-element Rx array can be viewed as composed of the contributions of multiple sub-scatterers:

$$\boldsymbol{Y}(t)=\Big[\sum_{\ell=1}^{L} a_\ell(t)\boldsymbol{c}(\boldsymbol{\Omega}_\ell)\Big]\cdot s(t)+\boldsymbol{W}(t),\ t=t_1,\ldots,t_N. \quad (1)$$

The components of the M-dimensional (M-D) complex vector $\boldsymbol{Y}(t)$ denote the M output signals of the Rx array at time t, $s(t)$ denotes the complex envelope of the transmitted signal, and the noise vector $\boldsymbol{W}(t)$ is a spatially and temporally white M-D Gaussian process with component variance σ_w^2. We assume that totally N observation samples are collected at time instances t_n, $n=1,\ldots,N$. Moreover in (1) ℓ denotes the index of the sub-scatterers with total number of L, while $a_\ell(t)$ and $\boldsymbol{\Omega}_\ell$ represent respectively, the complex gain and the DoA of the propagation path via the ℓth sub-scatterer. Finally, $\boldsymbol{c}(\boldsymbol{\Omega})=[c_1(\boldsymbol{\Omega}),\ldots,c_M(\boldsymbol{\Omega})]^{\mathrm{T}}$ with $[\cdot]^{\mathrm{T}}$ denoting transposition, is the response of the array. The direction $\boldsymbol{\Omega}$ ($=\boldsymbol{e}(\phi,\theta)$) is a unit vector uniquely determined by its spherical coordinates (ϕ,θ), where $\phi\in[-\pi,+\pi)$ and $\theta\in[0,\pi]$ denote respectively, the azimuth and the elevation. We assume $s(t)$ is known to the Rx. Without loss of generality $s(t)=1$.

A scatterer is called a SDS if $\phi_\ell=\bar{\phi}+\tilde{\phi}_\ell$ and $\theta_\ell=\bar{\theta}+\tilde{\theta}_\ell$ with $\tilde{\phi}_\ell$ and $\tilde{\theta}_\ell$ being small deviations from the NAoA $\bar{\phi}$ and the NEoA $\bar{\theta}$ respectively of the SDS. In this case, $\boldsymbol{c}(\boldsymbol{\Omega}_\ell)$ in (1) can be approximated by its first-order Taylor series expansion at the NDoA $\bar{\boldsymbol{\Omega}}=\boldsymbol{e}(\bar{\phi},\bar{\theta})$. Inserting the Taylor approximation for each $\boldsymbol{c}(\boldsymbol{\Omega}_\ell)$ in (1) yields the GAM model [3]

$$\begin{aligned}\boldsymbol{Y}(t)&=\sum_{\ell=1}^{L} a_\ell(t)[\boldsymbol{c}(\bar{\boldsymbol{\Omega}})+\tilde{\phi}_\ell\boldsymbol{c}_\phi^{'}(\bar{\boldsymbol{\Omega}})+\tilde{\theta}_\ell\boldsymbol{c}_\theta^{'}(\bar{\boldsymbol{\Omega}})]+\boldsymbol{W}(t),\\ &=\alpha(t)\boldsymbol{c}(\bar{\boldsymbol{\Omega}})+\beta_\phi(t)\boldsymbol{c}_\phi^{'}(\bar{\boldsymbol{\Omega}})+\beta_\theta(t)\boldsymbol{c}_\theta^{'}(\bar{\boldsymbol{\Omega}})+\boldsymbol{W}(t), \quad (2)\end{aligned}$$

where $\boldsymbol{c}_\phi^{'}(\boldsymbol{\Omega})=\frac{1}{\sin(\theta)}\cdot\frac{\partial\boldsymbol{c}(\boldsymbol{\Omega})}{\partial\phi}$, $\boldsymbol{c}_\theta^{'}(\boldsymbol{\Omega})=\frac{\partial\boldsymbol{c}(\boldsymbol{\Omega})}{\partial\theta}$, $\alpha(t)\doteq\sum_{\ell=1}^{L}a_\ell(t)$, $\beta_\phi(t)\doteq\sum_{\ell=1}^{L}a_\ell(t)\tilde{\phi}_\ell$ and $\beta_\theta(t)\doteq\sum_{\ell=1}^{L}a_\ell(t)\tilde{\theta}_\ell$. Using matrix notation, (2) can be written as

$$\boldsymbol{Y}(t)=\boldsymbol{F}(\bar{\boldsymbol{\Omega}})\boldsymbol{\xi}(t)+\boldsymbol{W}(t)$$

with $\boldsymbol{F}(\bar{\boldsymbol{\Omega}})=[\boldsymbol{c}(\bar{\boldsymbol{\Omega}}),\boldsymbol{c}_\phi^{'}(\bar{\boldsymbol{\Omega}}),\boldsymbol{c}_\theta^{'}(\bar{\boldsymbol{\Omega}})]$ and $\boldsymbol{\xi}(t)=[\alpha(t),\beta_\phi(t),\beta_\theta(t)]^{\mathrm{T}}$.

We make the following assumptions regarding the random elements characterizing the SDS.

- The azimuth deviations $\tilde{\phi}_1,\ldots,\tilde{\phi}_L$ are zero-mean uncorrelated random variables and have identical variance $\sigma_{\tilde{\phi}}^2$. The elevation deviations $\tilde{\theta}_1,\ldots,\tilde{\theta}_L$ are also zero-mean uncorrelated random variables and have identical variance $\sigma_{\tilde{\theta}}^2$. Moreover $\mathrm{E}[\tilde{\theta}_\ell\tilde{\phi}_{\ell'}]=\rho_{\phi\theta}\sigma_{\tilde{\phi}}\sigma_{\tilde{\theta}}\delta_{\ell\ell'}$ with $\mathrm{E}[\cdot]$, $\rho_{\phi\theta}$ and δ denoting respectively the expectation operator, the correlation coefficient between $\tilde{\theta}_\ell$ and $\tilde{\phi}_\ell$, and the Kronecker delta function.
- The gain processes $a_1(t),\ldots,a_L(t)$ are uncorrelated complex zero-mean circularly-symmetric wide-sense stationary (WSS) processes with autocorrelation function $R_{a_\ell}(\tau)$. In addition these gain processes have equal power, i.e. $R_{a_1}(0)=\ldots=R_{a_L}(0)$.

Under the above assumptions the standard deviations $\sigma_{\tilde{\phi}}$ and $\sigma_{\tilde{\theta}}$ are equal to the AS and the ES respectively of the SDS. Practically, a scatterer is called SDS when its AS and ES are smaller than 10°. Moreover the AS, ES and AECC $\rho_{\phi\theta}$ determine with close accuracy the DS [4] of the SDS. In addition, $\alpha(t)$, $\beta_\phi(t)$ and $\beta_\theta(t)$ are complex circularly-symmetric zero-mean WSS processes with autocorrelation functions $R_\alpha(\tau)=\sum_{\ell=1}^{L}R_{a_\ell}(\tau)$, $R_{\beta_\phi}(\tau)=\sigma_{\tilde{\phi}}^2R_\alpha(\tau)$ and $R_{\beta_\theta}(\tau)=\sigma_{\tilde{\theta}}^2R_\alpha(\tau)$ respectively, and cross-correlation functions $R_{\alpha\beta_\theta}(\tau)=R_{\alpha\beta_\phi}(\tau)=0$, and $R_{\beta_\phi\beta_\theta}(\tau)=\sigma_{\tilde{\phi}}\sigma_{\tilde{\theta}}\rho_{\phi\theta}R_\alpha(\tau)$ respectively. The parameters $\sigma_{\tilde{\phi}}^2$, $\sigma_{\tilde{\theta}}^2$, and $\rho_{\phi\theta}$ can be calculated from the above identities to be

$$\sigma_{\tilde{\phi}}^2=\frac{\sigma_{\beta_\phi}^2}{\sigma_\alpha^2},\quad \sigma_{\tilde{\theta}}^2=\frac{\sigma_{\beta_\theta}^2}{\sigma_\alpha^2},\ \text{and}\ \rho_{\phi\theta}=\frac{R_{\beta_\phi\beta_\theta}(0)}{\sigma_{\tilde{\phi}}\sigma_{\tilde{\theta}}\sigma_\alpha^2}, \quad (3)$$

where $\sigma_{(\cdot)}^2=R_{(\cdot)}(0)$. In the paper we consider a time-variant environment and assume that $R_\alpha(|t_{n'}-t_n|)=0, n\neq n',\ n,n'=1,\ldots,N$, or equivalently that, $\alpha(t)$, $\beta_\phi(t)$ and $\beta_\theta(t)$ are white random sequences.

In a scenario with D SDSs, (2) can be extended to

$$\begin{aligned}\boldsymbol{Y}(t)\ &=\ \sum_{d=1}^{D}\alpha_d(t)\boldsymbol{c}(\bar{\boldsymbol{\Omega}}_d)+\beta_{\phi,d}(t)\boldsymbol{c}_\phi^{'}(\bar{\boldsymbol{\Omega}}_d)\\ &\quad+\beta_{\theta,d}(t)\boldsymbol{c}_\theta^{'}(\bar{\boldsymbol{\Omega}}_d)+\boldsymbol{W}(t),\quad t=t_1,\ldots,t_N, \quad (4)\end{aligned}$$

where d denotes the indexing variable for the SDSs and $\bar{\boldsymbol{\Omega}}_d=\boldsymbol{e}(\bar{\phi}_d,\bar{\theta}_d)$.

III. The SAGE algorithm and the DS estimator

In a multi-SDS scenario as depicted by (4), the unknown parameter vector is

$$\begin{aligned}\boldsymbol{\theta}\doteq[&\sigma_w^2,\bar{\phi}_d,\bar{\theta}_d,\alpha_d(t),\beta_{\phi,d}(t),\beta_{\theta,d}(t);\\ &d=1,\ldots,D,\ t=t_1,\ldots,t_N].\end{aligned}$$

We choose the subsets of parameters updated in the iterations of the SAGE algorithm to be the sets including the parameters characterizing the signals contributed by the individual SDSs and the unknown noise variance. Hence, at Iteration $i = 1, 2, \ldots,$ $\boldsymbol{\theta}_d \doteq [\sigma_w^2, \bar{\phi}_d, \bar{\theta}_d, \alpha_d(t), \beta_{\phi,d}(t), \beta_{\theta,d}(t), t = t_1, \ldots, t_N]$ with $d = [(i-1) \mod D] + 1$ is updated. The admissible hidden-data [8] associated with $\boldsymbol{\theta}_d$ reads

$$\begin{aligned} \boldsymbol{X}_d(t) &= \alpha_d(t)\boldsymbol{c}(\bar{\boldsymbol{\Omega}}_d) + \beta_{\phi,d}(t)\boldsymbol{c}_\phi^{'}(\bar{\boldsymbol{\Omega}}_d) \\ &\quad + \beta_{\theta,d}(t)\boldsymbol{c}_\theta^{'}(\bar{\boldsymbol{\Omega}}_d) + \boldsymbol{W}(t), \quad t = t_1, \ldots, t_N. \end{aligned} \tag{5}$$

At Iteration i of the SAGE algorithm the objective function

$$Q(\boldsymbol{\theta}_d|\hat{\boldsymbol{\theta}}^{[i-1]}) \doteq \mathrm{E}\big[\Lambda(\boldsymbol{\theta}_d; \boldsymbol{X}_d)|\boldsymbol{Y}(t) = \boldsymbol{y}(t), \hat{\boldsymbol{\theta}}^{[i-1]})\big]$$

is computed in the expectation (E-) step. In the above expression $\hat{\boldsymbol{\theta}}^{[i-1]}$ denotes the estimate of $\boldsymbol{\theta}$ at the $(i-1)$th iteration. It can be shown that

$$\begin{aligned} Q(\boldsymbol{\theta}_d|\hat{\boldsymbol{\theta}}^{[i-1]}) &= -MN \ln \sigma_w^2 \\ &\quad - \tfrac{1}{\sigma_w^2} \sum_{t=t_1}^{t_N} \|\hat{\boldsymbol{x}}_d^{[i-1]}(t) - \boldsymbol{F}(\bar{\boldsymbol{\Omega}}_d)\boldsymbol{\xi}_d(t)\|^2, \end{aligned} \tag{6}$$

where

$$\begin{aligned} \hat{\boldsymbol{x}}_d^{[i-1]}(t) &= \boldsymbol{y}(t) - \sum_{d'=1, d'\neq d}^{D} \boldsymbol{F}(\hat{\bar{\boldsymbol{\Omega}}}_{d'}^{[i-1]})\hat{\boldsymbol{\xi}}_{d'}^{[i-1]}(t), \\ &\qquad t = t_1, \ldots, t_N \end{aligned} \tag{7}$$

is an estimate of $\boldsymbol{X}_d(t)$ given $\boldsymbol{y}(t)$ and assuming $\boldsymbol{\theta} = \hat{\boldsymbol{\theta}}^{[i-1]}$.

In the maximization (M-) step of the ith iteration $\hat{\boldsymbol{\theta}}_d^{[i]} = \arg\max_{\boldsymbol{\theta}_d}\{Q(\boldsymbol{\theta}_d|\hat{\boldsymbol{\theta}}^{[i-1]})\}$ is computed. Using a separable solution proposed in [9] the multiple-dimensional maximization operation reduces to a two-dimensional maximization problem

$$(\hat{\bar{\phi}}_d^{[i]}, \hat{\bar{\theta}}_d^{[i]}) = \arg \max_{(\bar{\phi}_d, \bar{\theta}_d)} \{\mathrm{tr}[\Pi_{\boldsymbol{F}(\bar{\boldsymbol{\Omega}}_d)} \hat{\boldsymbol{\Sigma}}_{\boldsymbol{x}_d^{[i-1]}\boldsymbol{x}_d^{[i-1]}}]\} \tag{8}$$

and

$$\begin{aligned} \hat{\boldsymbol{\xi}}_d^{[i]}(t) &= \boldsymbol{F}(\hat{\bar{\boldsymbol{\Omega}}}_d^{[i]})^{\dagger}\hat{\boldsymbol{x}}_d^{[i-1]}(t), \ t = t_1, \ldots, t_N, \\ (\widehat{\sigma_w^2})^{[i]} &= \tfrac{1}{NM}\mathrm{tr}[\Pi^{\perp}_{\boldsymbol{F}(\hat{\bar{\boldsymbol{\Omega}}}_d^{[i]})}\hat{\boldsymbol{\Sigma}}_{\boldsymbol{x}_d^{[i-1]}\boldsymbol{x}_d^{[i-1]}}], \end{aligned}$$

where $\mathrm{tr}[\cdot]$ denotes the trace operation, $\Pi_{\boldsymbol{F}(\bar{\boldsymbol{\Omega}}_d)} = \boldsymbol{F}(\bar{\boldsymbol{\Omega}}_d)\boldsymbol{F}(\bar{\boldsymbol{\Omega}}_d)^{\dagger}$ stands for the projection operator onto the column space of $\boldsymbol{F}(\bar{\boldsymbol{\Omega}}_d)$, $\boldsymbol{F}(\bar{\boldsymbol{\Omega}}_d)^{\dagger} \doteq \big[\boldsymbol{F}(\bar{\boldsymbol{\Omega}}_d)^{\mathrm{H}}\boldsymbol{F}(\bar{\boldsymbol{\Omega}}_d)\big]^{-1}\boldsymbol{F}(\bar{\boldsymbol{\Omega}}_d)^{\mathrm{H}}$ with $[\cdot]^{\mathrm{H}}$ denoting Hermitian transposition, is the pseudo-inverse of $\boldsymbol{F}(\bar{\boldsymbol{\Omega}}_d)$, $\hat{\boldsymbol{\Sigma}}_{\boldsymbol{x}_d^{[i-1]}\boldsymbol{x}_d^{[i-1]}} = \frac{1}{N}\sum_{t=t_1}^{t_N}\hat{\boldsymbol{x}}_d^{[i-1]}(t)\big(\hat{\boldsymbol{x}}_d^{[i-1]}(t)\big)^{\mathrm{H}}$, and $\hat{\bar{\boldsymbol{\Omega}}}_d^{[i]} = \boldsymbol{e}(\hat{\bar{\phi}}_d^{[i]}, \hat{\bar{\theta}}_d^{[i]})$.

In our implementation of the SAGE algorithm, the two-dimensional maximization in (8) is replaced by a coordinate-wise updating procedure similar to that used in [8]:

$$\begin{aligned} \hat{\bar{\phi}}_d^{[i]} &= \arg\max_{\bar{\phi}_d}\{\mathrm{tr}[\Pi_{\boldsymbol{F}\left(\boldsymbol{e}(\bar{\phi}_d, \hat{\bar{\theta}}_d^{[i-1]})\right)}\hat{\boldsymbol{\Sigma}}_{\boldsymbol{x}_d^{[i-1]}\boldsymbol{x}_d^{[i-1]}}]\}, \\ \hat{\bar{\theta}}_d^{[i]} &= \arg\max_{\bar{\theta}_d}\{\mathrm{tr}[\Pi_{\boldsymbol{F}\left(\boldsymbol{e}(\hat{\bar{\phi}}_d^{[i]}, \bar{\theta}_d)\right)}\hat{\boldsymbol{\Sigma}}_{\boldsymbol{x}_d^{[i-1]}\boldsymbol{x}_d^{[i-1]}}]\}. \end{aligned}$$

This procedure is still consistent with the SAGE framework with the admissible hidden-data given in (5). As a consequence the resulting iterative scheme exhibits the monotonicity property [8].

In the initialization step, the initial estimates $\hat{\boldsymbol{\theta}}_d^{[0]}$, $d = 1, \ldots, D$, are computed by means of a successive interference cancellation method similar to that used in [8].

From (3) sensible estimators of $\sigma_{\tilde{\phi}_d}$, $\sigma_{\tilde{\theta}_d}$ and $\rho_{\phi\theta}$ read

$$\hat{\sigma}_{\tilde{\phi}_d} = \sqrt{\widehat{\sigma^2_{\beta_{\phi,d}}}/\widehat{\sigma^2_{\alpha_d}}}, \tag{9}$$

$$\hat{\sigma}_{\tilde{\theta}_d} = \sqrt{\widehat{\sigma^2_{\beta_{\theta,d}}}/\widehat{\sigma^2_{\alpha_d}}}, \tag{10}$$

$$\hat{\rho}_{\phi\theta_d} = \hat{R}_{\beta_{\phi,d}\beta_{\theta,d}}(0)/(\hat{\sigma}_{\tilde{\phi}_d}\hat{\sigma}_{\tilde{\theta}_d}\widehat{\sigma^2_{\alpha_d}}) \tag{11}$$

respectively. The parameter $\widehat{\sigma^2_{\alpha_d}}$, $\widehat{\sigma^2_{\beta_{\phi,d}}}$ and $\widehat{\sigma^2_{\beta_{\theta,d}}}$ can be computed from the estimates of $\alpha_d(t)$, $\beta_{\phi,d}(t)$ and $\beta_{\theta,d}(t)$, $t = t_1, \ldots, t_N$ returned by the GAM-SAGE algorithm.

Notice that in a scenario with an unknown transmitted signal $s(t)$ the estimators (9)-(11) still apply. In this case the parameters $\alpha(t)$, $\beta_\phi(t)$ and $\beta_\theta(t)$ in (2) need merely to be redefined as $\alpha(t) \doteq \sum_{\ell=1}^{L} a_\ell(t)s(t)$, $\beta_\phi(t) \doteq \sum_{\ell=1}^{L} a_\ell(t)\tilde{\phi}_\ell s(t)$ and $\beta_\theta(t) \doteq \sum_{\ell=1}^{L} a_\ell(t)\tilde{\theta}_\ell s(t)$.

IV. Simulation Studies

The performance of the NDoA estimators using the GAM-SAGE algorithm is assessed by means of Monte-Carlo simulations first in a single-SDS scenario and then in a two-SDS scenario. The environment is time-variant, and $N = 20$ observation samples are considered in each Monte-Carlo run. Totally 200 runs are collected for calculating the root mean square estimation error (RMSEE) and the average estimation error (AEE) of the NDoA, AS, ES and AECC of the SDS. For comparison purpose the performance of the SAGE algorithm derived with the SS model (SS-SAGE) and the Spread-ESPRIT technique [6] is reported as well.

In the simulations, the Rx is equipped with a uniform 4×4 planar array consisting of 16 isotropic antennas. The spacing between adjacent elements is equal to half a wavelength. Each SDS consists of $L = 50$ sub-scatterers. The random elements characterizing the sub-scatterer contributions to the received signal are generated in such a way that the model assumptions described in the two bullet points given in Sect.III hold. In particular, the AoAs and EoAs of the sub-scatterers are independent, identically von-Mises distributed random variables centered around the SDS NAoA and NEoA respectively. Moreover the complex gains of the propagation paths via the sub-scatterers have equal amplitude.

Notice that the Spread-ESPRIT technique is applicable with ULAs only. Thus, when estimating the NAoAs of the SDSs the planar array is partitioned into 4 linear (row) sub-arrays. The Spread-ESPRIT technique first returns 4 NAoA estimates using these sub-arrays. The final estimate is the average of the 4 values. The NEoA estimation is carried out similarly.

In the single-SDS scenario both the NAoA and the NEoA of the SDS are set equal to $110°$. The AS and the ES are identical and range from $0.1°$ to $7°$. The SNR at the output of the estimators, which we denote by γ_o, varies from 0 dB to 30 dB. Fig. 1 depicts the RMSEE of the NAoA versus the output SNR with zero AECC and AS equal to $3°$ and $7°$. It can be observed that the GAM-SAGE algorithm outperforms the Spread-ESPRIT technique within the range $\gamma_o > 1$ dB. Both algorithms perform better than the SS-SAGE algorithm beyond a certain SNR threshold which depends on the AS and ES of the SDS and the estimators. These observations remain valid for other choice of the AS and the AECC.

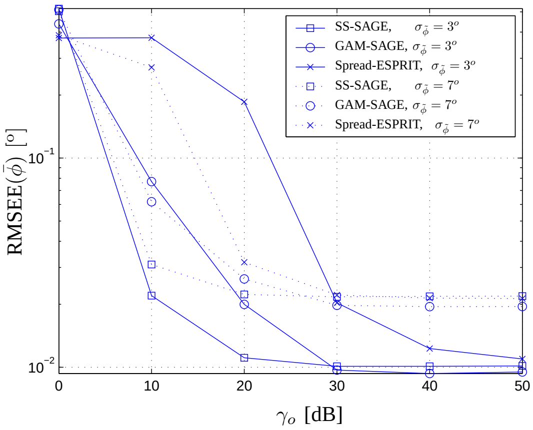

Fig. 1. RMSEE($\bar{\phi}$) vs. output SNR γ_o with $\sigma_{\bar{\phi}} = 3°$ and $7°$.

Investigations [5] of the AS estimator applied with a ULA show that the AS estimator is biased and returns large RMSEE regardless of the AS. This bias results due to the mismatch between the GAM model and the true signal model. It is also found that by adaptively selecting the array size for individual SDS, the approximation accuracy of the GAM model can be increased [5]. As a consequence, the bias and the RMSEE of the AS estimator can be reduced. The reader is referred to [5] for further information on the adaptive array-size selection technique.

Fig. 2 (a) and (b) depict respectively the AEE and the RMSEE of the AECC versus its true value with output SNR as a parameter. The AS and ES of the SDS are identical and equal to $1°$. The AECC ranges from 0.1 to 0.9. It can be observed that both the absolute AEE and the RMSEE of AECC decrease when the SNR increases. For $\gamma_o = 30$ dB the absolute AEE increases along with the absolute value of the AECC. These behaviors of the AEE are consistent with a theoretical analysis which shows that, in a noisy environment the AECC estimator returns estimates with absolute value smaller than the true value, and additionally, the absolute AEE increases when the absolute AECC increases, and also when the SNR decreases. Hence, to estimate AECC with an effective accuracy, high SNRs are necessary. For example, in Fig. 2 we observed that with $\gamma_o = 50$ dB, the AEE of AECC is confined within the range $[-0.05, 0.05]$, i.e. the estimator is nearly unbiased, and the returned RMSEE is roughly around 0.15. As the accuracy of the AECC estimate depends on the GAM approximation accuracy in describing the signal contribution of the SDS, it is conjectured that the performance of the AECC estimator can be improved by applying the array-size selection technique [5].

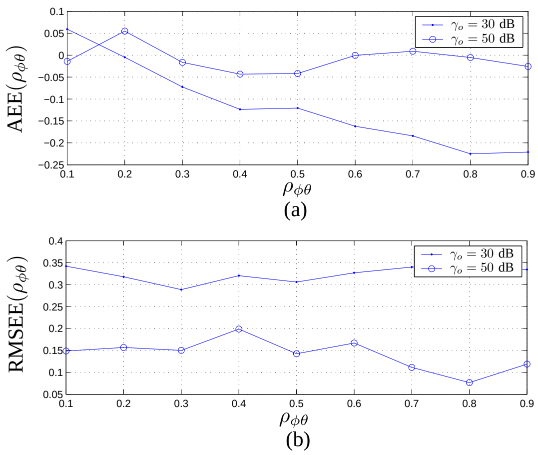

Fig. 2. AEE($\rho_{\phi\theta}$), (a) and RMSEE($\rho_{\phi\theta}$), (b) vs. the true value with the output SNR γ_o as a parameter.

In the two-SDS scenario, the SDS of interest (SDS_1) has fixed NAoA and NEoA, both being equal to $110°$. The NEoA of the second SDS (SDS_2) equals the NEoA of SDS_1. The NAoA spacing $\Delta\bar{\phi}$ between SDS_1 and SDS_2 ranges from $5°$ to $70°$. The two SDSs have identical AS and ES equal to $5°$, and their AECCs are equal to zero. The output SNRs for SDS_1 and SDS_2 are 20 dB and 29 dB respectively, i.e. we consider a situation with a strong SDS power unbalance of 9 dB. Fig. 3 (a) and Fig. 3 (b) depict respectively the AEE and the RMSEE of the NAoA $\bar{\phi}_1$ for the weaker SDS (SDS_1) versus $\Delta\bar{\phi}$. Notice that the Spread-ESPRIT technique is inapplicable in estimating the NDoAs for two SDSs because of the insufficient number of point scatterer estimates that can be computed using a 4-element ULA [6]. The performance of the Spread-ESPRIT technique in a two-SDS scenario using an 8-element ULA is reported and compared with that of the SAGE algorithm in [10], to which the reader is referred for more information. Each element of the pair of NAoA estimates, say $(\hat{\bar{\phi}}', \hat{\bar{\phi}}'')$ computed by the SAGE algorithm is assigned to one of the two SDSs

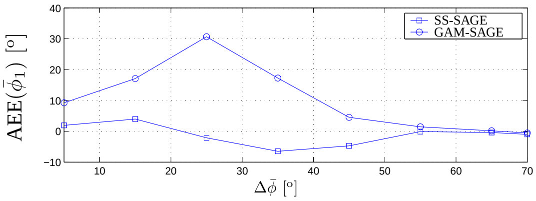

(a)

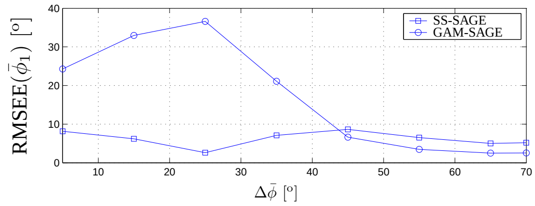

(b)

Fig. 3. AEE($\bar{\phi}_1$) (a) and RMSEE($\bar{\phi}_1$) (b) vs. the NAoA spacing $\Delta\bar{\phi}$ of the two SDSs.

according to

$$(\hat{\bar{\phi}}_1, \hat{\bar{\phi}}_2) = \arg \min_{\substack{(\phi',\phi'')\in \\ \{(\hat{\bar{\phi}}',\hat{\bar{\phi}}''),(\hat{\bar{\phi}}'',\hat{\bar{\phi}}')\}}} \|(\phi',\phi'') - (\bar{\phi}_1, \bar{\phi}_2)\|,$$

where $\|\cdot\|$ is the Euclidean norm.

It can be observed that the SS-SAGE algorithm performs better than the GAM-SAGE algorithm in terms of lower AEEs and RMSEEs when $\Delta\bar{\phi} < 45°$. When $\Delta\bar{\phi} \geq 45°$, the GAM-SAGE algorithm outperforms the SS-SAGE algorithm, and its RMSEE stabilizes at $2.5°$ when $\Delta\bar{\phi} \geq 55°$. The poor performance of the GAM-SAGE algorithm when the separation is small is due to the fact that the GAM-SAGE cannot separate the SDSs when the NAoA spacing is less than a certain threshold, e.g. $55°$ from the simulation results. Notice that $55°$ equals twice the intrinsic azimuth resolution of the 4-element ULA [8]. Although the SS-SAGE algorithm outperforms the GAM-SAGE algorithm at small direction separation, its RMSEE remains roughly equal to $8°$ regardless of the separation. These observations show that provided the NAoA spacing equals twice the intrinsic azimuth resolution of the array, the GAM-SAGE algorithm returns the RMSEE within a tolerably low level in estimating weaker SDSs. Moreover provided the above condition occurs, the GAM-SAGE algorithm in estimating the NAoA of the weaker SDS is more robust towards the impact of the stronger SDS than the SS-SAGE algorithm.

V. Conclusions

In this paper, the SAGE (Subspace-Alternating Generalized Expectation-maximization) algorithm [1] [2] is derived based on a deterministic version of the generalized array manifold (GAM) model proposed in [3] to estimate the nominal directions, i.e. azimuths and elevations of slightly distributed scatterers (SDSs) in time-variant environments. As byproducts estimates of the azimuth spreads (ASs), elevation spread (ESs), as well as azimuth-elevation correlation coefficients (AECCs) of the SDSs can be computed from the estimates of the GAM parameters.

Simulation studies show that in a single-SDS scenario, the GAM-SAGE algorithm outperforms the Spread-ESPRIT technique [6], and both of them outperform the SAGE algorithm derived with the conventional specular-scatterer (SS) model (SS-SAGE) when the output SNR is beyond a certain threshold, which depends on the AS and ES of the SDS.

In the two-SDS scenario with strong power unbalance between the SDSs, the direction separation of these SDSs needs to be at least larger than twice the intrinsic resolution of the used array in order for the GAM-SAGE estimator to return direction estimates with a tolerable accuracy. The SS-SAGE is more robust towards bias for low direction separation but performs poor in terms of root mean squared estimation error (RMSEE).

The AS and ES estimators are found to be biased and return large estimation errors. Their performance can be improved by applying an array-size selection technique proposed in [5]. The AECC estimator is found to be biased in noisy environments. The output SNR needs to be 50 dB for this estimator to be nearly unbiased and exhibit tolerably small RMSEE. It is conjectured that the performance of the AECC estimator can be improved by applying the array-size selection technique [5].

The proposed estimators can be applied with arbitrary arrays. They can also be used in time-invariant environments with only a slight modification. Their extension to include the nominal directions and direction spreads of the SDSs at both Tx and Rx sites in a MIMO system is straightforward.

References

[1] J. A. Fessler and A. O. Hero, "Space-alternating generalized expectation-maximization algorithm," *IEEE Trans. Signal Processing*, vol. 42, no. 10, pp. 2664–2677, Oct. 1994.

[2] B. H. Fleury, M. Tschudin, R. Heddergott, D. Dahlhaus, and K. L. Pedersen, "Channel parameter estimation in mobile radio environments using the SAGE algorithm," *IEEE Journal on Selected Areas in Communications*, vol. 17, no. 3, pp. 434–450, Mar. 1999.

[3] D. Asztély, B. Ottersen, and A. L. Swindlehurst, "A generalized array manifold model for local scattering in wireless communications," *Proc. IEEE Int. Conf. Acoust., Speach, Signal Processing, ICASSP '97*, 1997.

[4] B. H. Fleury, "First- and second-order characterization of direction dispersion and space selectivity in the radio channel," *IEEE Trans. Information Theory*, no. 6, pp. 2027–2044, Sept. 2000.

[5] X. Yin and B. Fleury, "Angular spread estimation for slightly distributed scatterers using the generalized array manifold model," *International ITG/IEEE Workshop on Smart Antennas, WSA 2005, Duisburg*, May 2005, accepted paper.

[6] M. Bengtsson and B. Ottersten, "Low-complexity estimators for distributed sources," *IEEE Trans. Signal Processing*, vol. 48, no. 8, pp. 2185–2194, Aug. 2000.

[7] D. Asztély and B. Ottersten, "The effects of local scattering on direction of arrival estimation with MUSIC and ESPRIT," *Proc. IEEE Int. Conf. Acoust., Speach, Signal Processing, ICASSP '98,*, vol. 6, pp. 3333–3336, May 1998.

[8] B. H. Fleury *et. al.*, "Channel parameter estimation in mobile radio environments using the SAGE algorithm," *IEEE Journal on Selected Areas in Communications*, vol. 17, no. 3, pp. 434–450, Mar. 1999.

[9] A. G. Jaffer, "Maximum likelihood direction finding of stochastic sources: a separable solution," *Proc. IEEE Int. Conf. Acoust., Speach, Signal Processing, ICASSP '88*, vol. 5, pp. 2893–2896, 1988.

[10] X. Yin and B. H. Fleury, "Nominal direction estimationfor slightly distributed scatterers using the sage algorithm," *Submitted to 2005 IEEE AP-S International Symposium and USNC/URSI national radio science meeting, AP-S/URSI, Washington DC, USA*, 2005.